Original Article

ASPM and *TROAP* gene expression as potential malignant tumor markers

Han Liu[1,2#], Qiuxiang Zhou[3#], Xiang Xu[1,2], Yanhua Du[4], Jun Wu[1,2,5]

[1]Department of Laboratory Medicine, Jiading Branch of Shanghai General Hospital, Shanghai Jiao Tong University School of Medicine, Shanghai, China; [2]Department of Pathology, The Affiliated Hospital of Youjiang Medical University for Nationalities, Baise, China; [3]Department of Emergency and Critical Care, Shanghai Changzheng Hospital, Naval Military Medical University, Shanghai, China; [4]Department of Gynecology, Obstetrics and Gynecology Hospital of Fudan University, Shanghai, China; [5]The Key Laboratory of Molecular Pathology (Hepatobiliary Diseases) of Guangxi, Baise, China

Contributions: (I) Conception and design: H Liu, Y Du, J Wu; (II) Administrative support: Y Du, J Wu; (III) Provision of study materials or patients: H Liu, Q Zhou; (IV) Collection and assembly of data: H Liu, Q Zhou; (V) Data analysis and interpretation: H Liu, X Xu, J Wu; (VI) Manuscript writing: All authors; (VII) Final approval of manuscript: All authors.

[#]These authors contributed equally to this work.

Correspondence to: Dr. Jun Wu. Department of Laboratory Medicine, Jiading Branch of Shanghai General Hospital, Shanghai Jiao Tong University School of Medicine, Shanghai 201803, China. Email: jun.wu@shsmu.edu.cn; Dr. Yanhua Du. Department of Gynecology, Obstetrics and Gynecology Hospital of Fudan, Shanghai 200011, China. Email: yanhdu@163.com.

Background: Although increasing evidence supports a vital role for assembly factor for spindle microtubules (ASPM) and trophinin-associated protein (TROAP) in the tumorigenesis of some cancers, no systematic pancancer analyses of ASPM and TROAP have been performed. Thus, we aimed to investigate the potential functions of ASPM and TROAP across 31 cancer types.

Methods: Based on datasets from The Cancer Genome Atlas (TCGA), Human Protein Atlas (HPA), GeneCloud of Biotechnology Information (GCBI) and Gene Expression Omnibus (GEO), we employed an array of bioinformatics methods to explore the potential oncogenic roles of ASPM and TROAP.

Results: ASPM and TROAP, which were highly expressed in most cancers and presented a strict positive correlation, led to a decreased life expectancy among cancer patients. ASPM and TROAP both regulated cell replication in the S&G2 phase of the cell cycle. Through a protein-protein interaction network (PPI) analysis of ASPM and TROAP, we found that cell division cycle 20 (CDC20) was regulated by TROAP and functioned upstream of ASPM. Thus, TROAP can regulate the role of ASPM in cancers.

Conclusions: The ASPM and TROAP have a significant positive correlation and similar expression profiles, and promote tumor malignancy and development in the S&G2 phase of the cell cycle. Since ASPM is one of the downstream targets of TROAP, TROAP and especially ASPM may be potential tumor makers and promising targets for therapeutic strategy.

Keywords: Assembly factor for spindle microtubules (ASPM); trophinin-associated protein (TROAP); pancancer; cell division cycle 20 (CDC20); cell cycle

Submitted Jan 07, 2022. Accepted for publication May 20, 2022.
doi: 10.21037/atm-22-1112
View this article at: https://dx.doi.org/10.21037/atm-22-1112

Introduction

As life expectancy increases, cancers are gradually surpassing cardiovascular diseases as a major risk factor for human health and the most common cause of death in China (1). However, there are still no effective strategies for cancer therapy (2). One convenient approach to find potential therapy targets is pancancer expression analysis of genes in

public databases, such as TCGA and HPA, to evaluate their correlations with clinical prognosis and relevant signaling pathways in cancer (3-5).

Assembly factor for spindle microtubules (*ASPM*) is overexpressed in a variety of cancer cell lines, including colorectal cancer, breast cancer and gastric cancer (6-8). A previous study suggested that the *ASPM*-katanin complex regulated microtubule disassembly at spindle poles (9). Furthermore, downregulation of *ASPM* could arrest the cell cycle of glioblastoma multiforme (GBM) cells and attenuate Wnt/β-catenin signaling activity in GBM (10). *ASPM* serves as an oncogenic regulator of tumor cell proliferation and metastasis in lung carcinoma (7). However, the role of *ASPM* in tumors remains elusive.

Trophinin-associated protein (*TROAP*), also known as tastin, is involved in centrosome integrity and spindle assembly during mitosis (11). *TROAP* promotes tumorigenesis and predicts poor prognosis in prostate cancer, breast cancer and hepatocellular carcinoma (HCC) (12-14). However, *TROAP* was also reported to suppress cellular growth and migration in HCC (15), which indicated the intricate mechanism of *TROAP* in tumor progression. In general, the biological functions of *TROAP* in cancer remain to be elucidated.

Cell division cycle 20 (CDC20), also called Fizzy, is a modulator of the ubiquitin E3 ligase anaphase promoting complex/cyclosome (APC/C). APC/C is well known for its role in regulating the mitotic transition from metaphase to anaphase (16). Recent evidence indicates that CDC20 is overexpressed in various cancers, such as prostate cancer, glioblastoma, and breast cancer (17-19). Furthermore, a previous study has reported the regulators of CDC20. For example, p53 inhibits tumor cell growth through the indirect regulation of CDC20 (20). USP44 (ubiquitin-specific protease 44) deubiquitinates CDC20 and blocks premature activation of APC by stabilizing the APC-inhibitory Mad2-CDC20 complex (21). CDC20 also promotes cell proliferation and invasion by regulating the Wnt/β-catenin signaling pathway in prostate cancer and cutaneous squamous cell carcinoma (22,23). In summary, increasing evidence suggests that CDC20 is an emerging oncogenic protein and that its expression can impact tumor patient prognosis.

In the present study, we reported that *ASPM* and *TROAP* were highly expressed in most cancers and predicted a poor prognosis among tumor patients. Meanwhile, these 2 genes presented a strict positive correlation. Mechanistically, *ASPM* and *TROAP* both regulated cell replication in the S&G2 phase of the cell cycle. As CDC20 is involved in the regulation of the cell cycle, we identified a new upstream regulator and downstream substrate of CDC20, *TROAP* and *ASPM*. Thus, *TROAP* regulates the role of *ASPM* in cancers, and *ASPM* is likely associated with cancer cell proliferation. Therefore, targeting *ASPM* may be a promising tumor therapeutic strategy for cancer patients. We present the following article in accordance with the STREGA reporting checklist (available at https://atm.amegroups.com/article/view/10.21037/atm-22-1112/rc).

Methods

Data processing and differential expression analysis

Raw data were downloaded from TCGA (containing 11,069 samples from 33 types of cancer). The downloaded data and expression levels were compared between cancer samples and matched standard samples in 31 cancers. Expression data were log2-transformed, and two sets of t tests were conducted on these tumor types; $P<0.05$ was considered to indicate differential expression between tumor and normal tissues. Data analysis was conducted using R software (Version 4.0.2; https://www.Rproject.org), and the R package "ggpubr" was used to draw box plots. The study was conducted in accordance with the Declaration of Helsinki (as revised in 2013).

Differentially expressed genes (DEGs)

The limma package of the R language package was used to screen the DEGs between cancer samples and normal samples. Adjusted $P<0.05$ and $|\log2\text{fold change (FC)}| >1$ were chosen as the cutoff criteria.

Comprehensive analysis of the PPI network

The Search Tool for the Retrieval of Interacting Genes Database (STRING) (https://cn.string-db.org/) was used to assess protein-protein interaction (PPI) information (24). In addition, to explore the relationship between DEGs, we used the STRING database and converted the results visually using Cytoscape software, a general-purpose, open-source software platform for network biology analysis and visualization (25). A confidence score >0.7 was set as significant.

Statistical analysis

All analyses were conducted three times and represented

Table 1 Differential expression of the 16 most expressed genes in 31 types of cancers

No.	Gene symbol	UP	DOWN	NS
1	*TROAP*	23	1	7
2	*ASPM*	22	1	8
3	*TICRR*	9	1	20
4	*GJB4*	8	1	22
5	*RAB27A*	4	4	23
6	*SYNDIG1*	4	4	23
7	*NLGN3*	2	6	23
8	*BCL2L14*	6	1	24
9	*SIX2*	5	1	25
10	*FBRSL1*	5	0	26
11	*PCDH19*	4	1	26
12	*CACNB4*	1	3	27
13	*LA16c-329F2.2*	0	1	30
14	*RP13-580B18.4*	0	1	30
15	*RP11-295P9.8*	0	0	31
16	*HSPA8P1*	0	0	31

UP, upregulation; DOWN, downregulation; NS, no significant.

data from three separate experiments. Two-tailed Student's t test was utilized to determine the significance of differences between subgroups. Statistical analysis was processed via SPSS 16.0. Statistical significance was set at probability values of $P<0.05$.

Results

ASPM and TROAP are relatively broad-spectrum malignant tumor markers

Prognostic factors are crucial indicators for tumor malignancy evaluation. We analyzed 31 cancer types and listed the top 10 genes in each cancer type related to poor prognosis based on the GEPIA results (Table S1) (http://gepia.cancer-pku.cn/). In *Table 1*, 16 genes that appeared more than once among the 31 cancer types were classified into upregulation (UP), no significant change (NS), and downregulation (DOWN) according to their expression levels. We found that *ASPM* and *TROAP* were significantly elevated in most cancer types (Figure S1, *Figure 1A,1B*), and the high expression of *ASPM* and *TROAP* led to a decreased life expectancy in cancer patients (*Figure 1C,1D*). High expression of both *ASPM* and *TROAP* appeared in 20/31 cancer types, while high expression of either *ASPM* or *TROAP* was represented in 5 more malignancies (64.52%) (*Figure 1E*). Therefore, *ASPM* and *TROAP* can be used as part of a broader spectrum of malignant tumor markers.

ASPM and TROAP are positively correlated in the tumor microenvironment

We analyzed the correlation between *ASPM* and *TROAP* in tumors. By measuring changes in their expression in various cancers, we found that these 2 genes often changed simultaneously (*Figure 2A*), suggesting that *ASPM* and *TROAP* play a role in specific types of cancer, thereby regulating tumorigenesis. We also analyzed the correlation between the expression levels of these genes. The results showed a high degree of identity (*Figure 2B*), with a statistical P value equal to 0. This suggests that, in most types of cancer, *ASPM* and *TROAP* show a strict positive correlation.

Based on these results, *ASPM* and *TROAP* can be used as indicators of malignant cancer, as they have a significant correlation with a decline in patient survival. In addition, the data showed that *ASPM* and *TROAP* have clear synchronicity in expression levels in multiple types of cancer. We analyzed the differences in the expression of *ASPM* and *TROAP* in different cancer stages and found that *ASPM* and *TROAP* is highly expressed in kidney chromophobe (KICH) with stage IV compared with other stages. Meanwhile, most tumors such as adrenocortical carcinoma (ACC) and kidney renal papillary cell carcinoma (KIRP) with stage III or stage IV presented relatively high *ASPM* and *TROAP* expression (*Figure 2C,2D*). This may be a cause of the significant reduction in survival rates of cancer patients. In addition, the synchronicity of expression between *ASPM* and *TROAP* was reflected in the significantly high expression of these genes in stage III and stage IV of cancer ($F>2$), with the exception of head and neck squamous cell carcinoma (HNSC) (*Figure 2E*). Therefore, *ASPM* and *TROAP* show a high degree of synchronization and may be related to the decline in survival rate in advanced stages of these cancers.

Clinicopathologic features of ASPM and TROAP

After analyzing the basic features of *ASPM* and *TROAP* using the GEPIA platform, we investigated the physiological characteristics of these genes. Because GEPIA is a resource

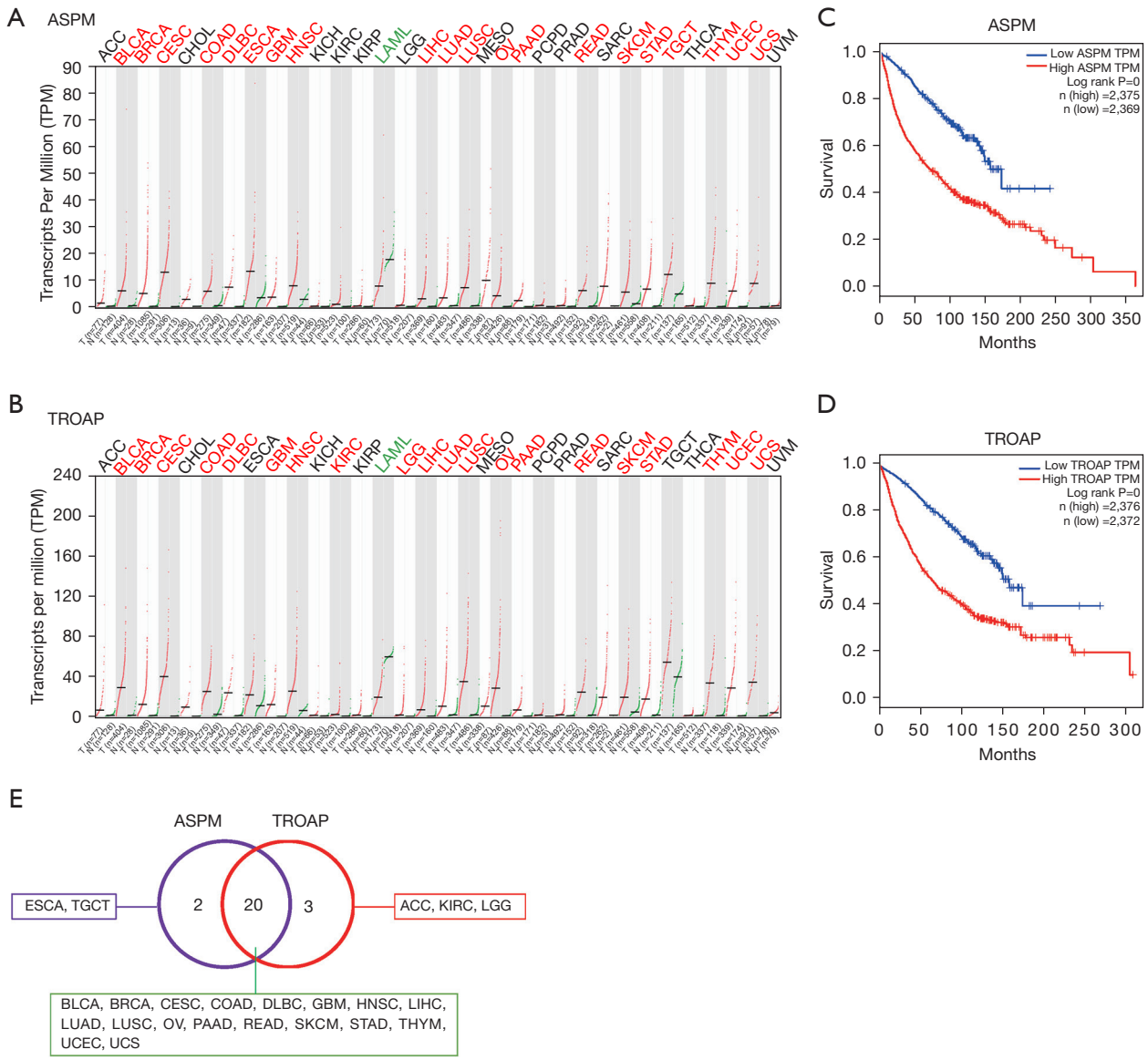

Figure 1 Expression of ASPM and TROAP in different cancers. (A,B) ASPM and TROAP expression analysis in various cancers. Tumors highlighted with red letters means the gene expression is significantly upregulated in tumor tissue. Tumors highlighted with green letters means the gene expression is significantly upregulated in normal tissue. Tumors highlighted with black letters means the gene expression change is not significant. (C,D) ASPM and TROAP poor prognosis analysis. (E) Venn diagram of significantly high expression of ASPM and TROAP. ASPM, assembly factor for spindle microtubules; TROAP, trophinin-associated protein.

for RNA data, the overall phenotypes of cancer significantly rely on protein expression. Therefore, we used the HPA database, which provides resources relating to the protein expression of genes under pathological conditions, such as cancer, to analyze the clinical and pathologic phenotypes of *ASPM* and *TROAP* (26-28).

We first analyzed the features of *ASPM* to identify its tissue-specific and cell-specific characteristics (*Figure 3A,3B*). The expression level of *ASPM* differed in various tissues, with high expression in bone marrow, lymph nodes, tonsils, testes, and other organs (*Figure 3A*). *ASPM* is also highly expressed in erythrocytes, spermatocytes, spermatogonia, extravillous trophoblasts, Hofbauer cells, cytotrophoblasts, basal keratinocytes, undifferentiated

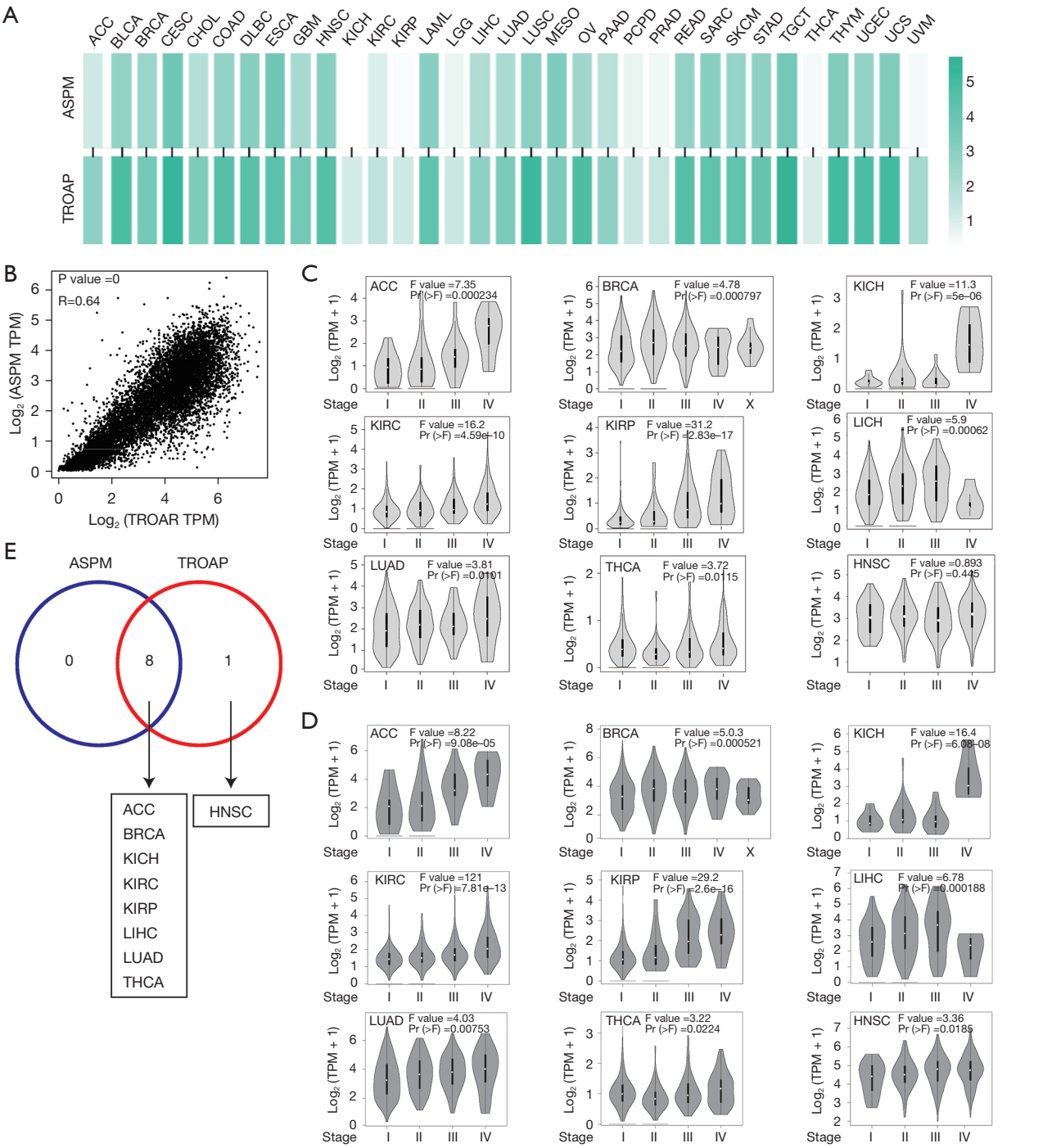

Figure 2 ASPM and TROAP correspond to changes in different cancer types. (A) Synchronous changes in the expression of ASPM and TROAP in various cancers. (B) Correlation of the overall expression of ASPM and TROAP. (C,D) The expression of ASPM and TROAP in several cancer stages. (E) Venn diagram of (C,D). ASPM, assembly factor for spindle microtubules; TROAP, trophinin-associated protein; Stage X, no clear stages.

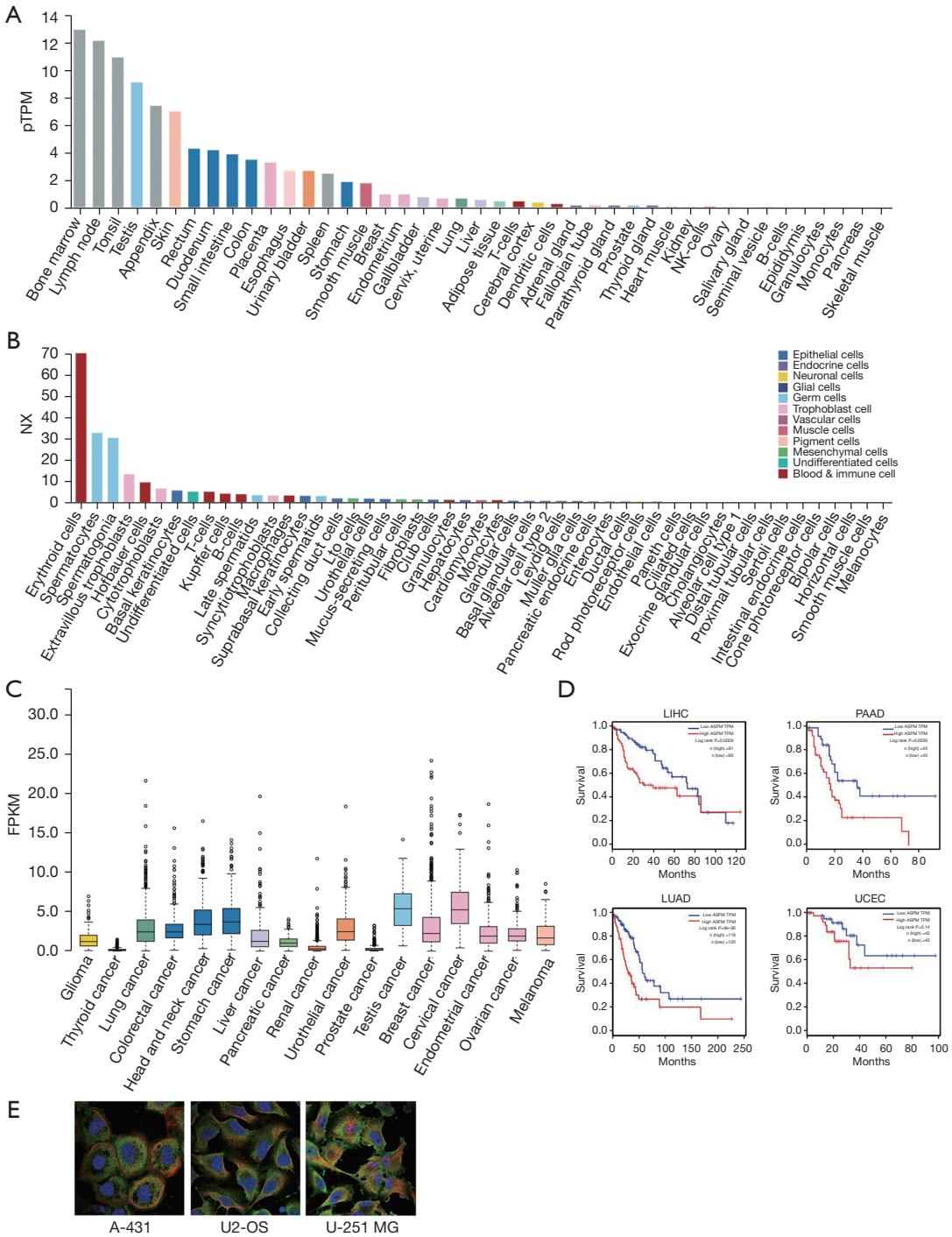

Figure 3 Expression of *ASPM* in various tissues, cancer species and cell lines. (A) The expression of *ASPM* in various tissues. (B) The expression of *ASPM* in various cell types. (C) The expression of *ASPM* in different cancers (based on HPA data and statistics of various tissue cancers). (D) *ASPM* and poor prognosis in 4 types of cancers. (E) Expression of APSM in 3 cell lines (immunofluorescence). The cells are imaged using a laser scanning confocal microscope with a 63x objective. Red represented microtubulin, green represented *ASPM* and blue represented nucleus. These images are available from v21.0.proteinatlas.org. (https://www.proteinatlas.org/ENSG00000066279-*ASPM*/subcellular#human). A-431, human skin squamous cell carcinoma; U2-OS, human osteosarcoma cells; U-251 MG, human glioma cells. *ASPM*, assembly factor for spindle microtubules; HPA, Human Protein Atlas.

cells, T cells, Kupffer cells, B cells, late-stage sperm cells, and other immune or male reproduction-related cells (*Figure 3B*). This suggests that high expression of *ASPM* may be involved in immune regulation in the tumor microenvironment. In consistent with *TROAP*, the expression level of *ASPM* among tumors also presented low cancer specificity (*Figure 3C*). We used HPA data to analyze the poor prognosis of 4 specific cancer types related to *ASPM*: liver hepatocellular carcinoma (LIHC), pancreatic adenocarcinoma (PAAD), lung adenocarcinoma (LUAD), and uterine corpus endometrial carcinoma (UCEC). The results showed that the high expression of *ASPM* was indeed associated with poor prognosis in these 4 cancer types (*Figure 3D*). Moreover, the immunofluorescence staining results of 3 cell lines (A-431: human skin squamous cell carcinoma; U2-OS: human osteosarcoma cells; and U-251 MG: human glioma cells) showed that *ASPM* is mainly expressed in the cytoplasmic matrix and interacts with cytoplasmic matrix microtubules (*Figure 3E*).

We used the same method of analysis to investigate *TROAP*. The data showed that *TROAP* and *ASPM* have similar tissue expression characteristics. That is, they are highly expressed in organs, such as testes, bone marrow, tonsils, and lymph nodes (*Figure 4A*). However, *TROAP* has its own cell-specific expression characteristics. *TROAP* is highly expressed in early sperm cells, late sperm cells, extravillous trophoblasts, spermatocytes, Hofbauer cells, spermatogonia, cytotrophoblasts, Ito cells, undifferentiated cells, basal keratinocytes, syncytiotrophoblast cells, Kupffer cells, T cells, mucus secreting cells, and other cells (*Figure 4B*). According to HPA data, the expression level of *TROAP* among tumors presented low cancer specificity (*Figure 4C*). Immunohistochemical staining showed discrepant protein levels of *TROAP* in liver cancer, lung cancer, breast cancer, prostate cancer, and colon cancer (*Figure 4D*). Therefore, based on protein levels, *TROAP* is closely related to the progression of malignant tumors. However, in terms of prognosis, the HPA database shows that *TROAP* leads to a poor prognosis only in LIHC (*Figure 4E*).

ASPM and TROAP regulate cell replication in the S&G2 phase

As the process of carcinogenesis is caused by an uncontrolled cell cycle, previously reported malignant cancer or tumor markers have been related to cell cycle regulation (29-31). The cell cycle is divided into 2 phases: interphase and division (32). Cancer cells also have a cell cycle, but their cycle regulation mechanism is destroyed (33), leading to uncontrolled cell growth and the transformation of normal cells into tumor cells. Using the GEPIA platform and the HPA database, we screened *ASPM* and *TROAP* as malignant tumor markers and analyzed their cell cycle changes.

We found that *TROAP* was more highly expressed than *ASPM* (*Figure 5A,5B*). The overall expression level of *ASPM* declined in the S transition (S-tr) period, but there was no significant difference between *TROAP* levels in the G1 and S-tr periods. *ASPM* and *TROAP* reached their highest expression levels in the S&G2 phase, but due to large variation within the group, the results were not significant. However, the S&G2 phase should still be considered the period when *ASPM* and *TROAP* play a role in cell cycle regulation. In the S&G2 phase, cell proliferation may become malignant due to an error in regulation, which eventually leads to cancer formation. Our results showed that *ASPM* and *TROAP* have very similar change profiles. Although the overall level of *TROAP* was still relatively high, there was a simultaneous rise and fall in the expression of both genes. This suggests that *ASPM* and *TROAP* may both regulate cell replication in the S&G2 phase of the cell cycle.

The interaction network of ASPM and TROAP

As *ASPM* and *TROAP* are highly correlated in a variety of cancers, we used the GCBI database to analyze the regulatory network of these 2 genes. The results showed that *ASPM* was mainly regulated by its interaction with proteins and less regulated by long non-coding RNA (lncRNA) and miRNA, while *TROAP* was mainly regulated by lncRNA (*Figure 6A,6B*). The regulatory factors shared by *ASPM* and *TROAP* were 2 miRNAs, namely hsa-miR-215-5p and hsa-miR-192-5p (*Figure 6C*). This finding suggests that these 2 miRNAs may be putative targets to weaken the functionality of *ASPM* and *TROAP*. In addition, we screened the potential TFs of *ASPM* and *TROAP* (*Figure 6D,6E*) and found that these genes may share 22 TFs (*Figure 6F*).

We performed a protein-protein interaction network (PPI) analysis of *ASPM* and *TROAP* (*Figure 6G,6H*). The results showed that *ASPM* is regulated by more factors than *TROAP*, which is consistent with previous reports (*Figure 6A-6F*). In addition, we found that CDC20 plays an important role in various regulatory factors. CDC20 is regulated by *TROAP* and is upstream of *ASPM*. Interestingly, *TROAP* itself can directly regulate *ASPM*;

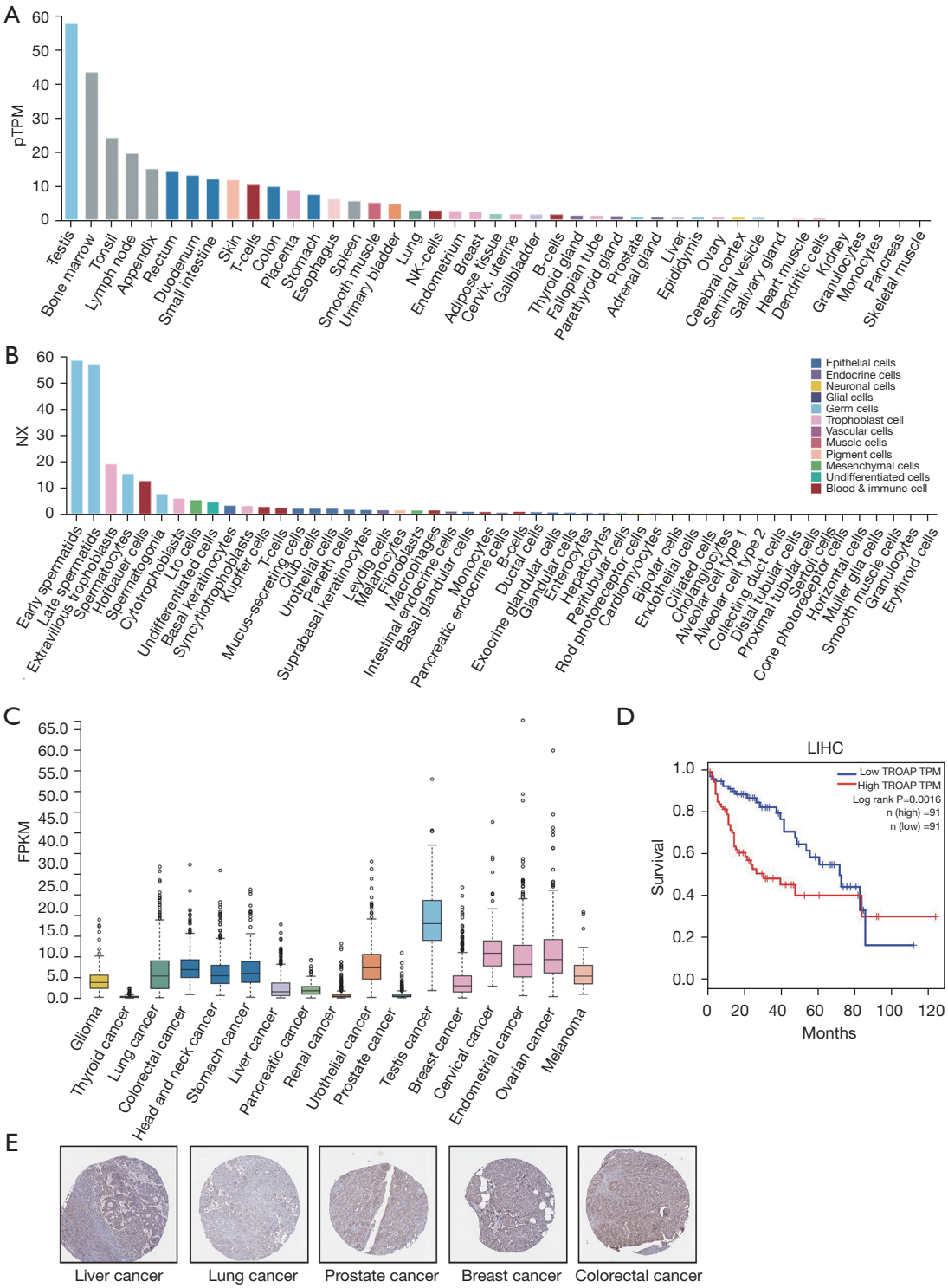

Figure 4 Expression of *TROAP* in various tissues, cancer species and cell lines. (A) *TROAP* expression in various tissues. (B) *TROAP* expression in various cell types. (C) *TROAP* expression in different cancers (based on HPA data and statistics of various tissue cancers). (D) *TROAP* and poor prognosis in LIHC. (E) *TROAP* expression in 5 types of cancer (immunohistochemistry). Magnification power: ×100. These images are available from v21.0.proteinatlas.org. (https://www.proteinatlas.org/ENSG00000135451-*TROAP*/pathology). *TROAP*, trophinin-associated protein; HPA, Human Protein Atlas; LIHC, liver hepatocellular carcinoma.

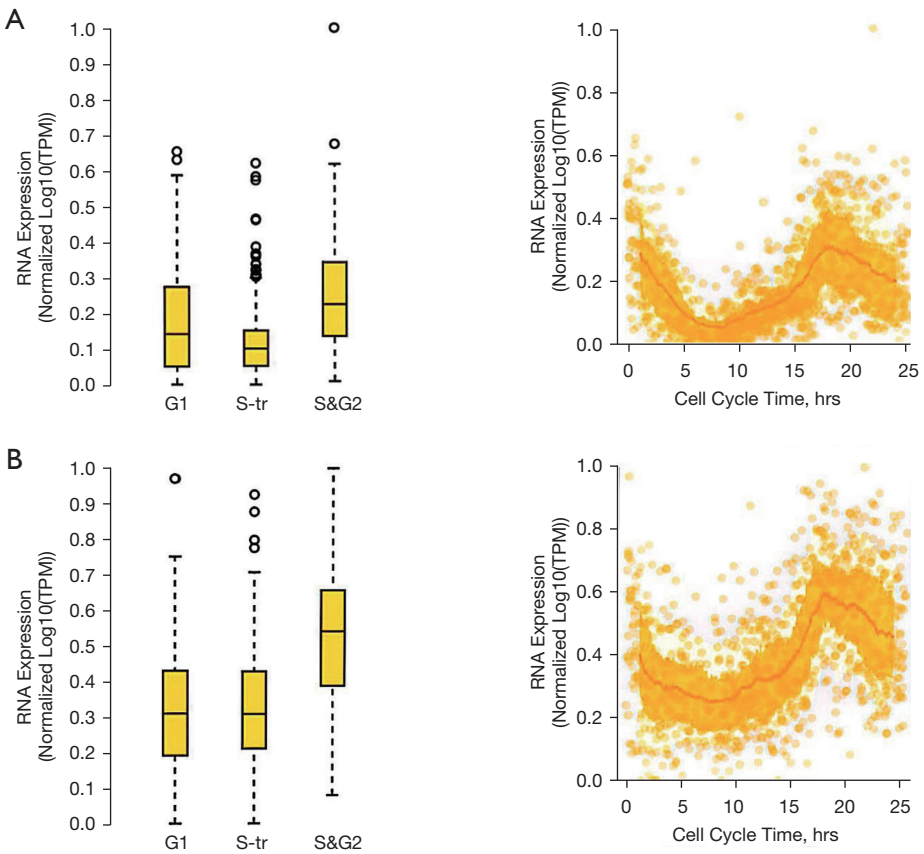

Figure 5 ASPM and TROAP correspond to cell cycle changes. Changes in *ASPM* (A) and *TROAP* (B) in different phases of the cell cycle. *ASPM*, assembly factor for spindle microtubules; *TROAP*, trophinin-associated protein. These images are available from v21.0.proteinatlas.org. (https://www.proteinatlas.org/ENSG00000135451-TROAP/subcellular#cell_cycle; https://www.proteinatlas.org/ENSG00000066279-ASPM/subcellular#cell_cycle).

that is, *ASPM* is also a downstream factor of *TROAP* (*Figure 6H*). Although *TROAP* is upstream of regulatory factors, such as DNA topoisomerase II alpha (TOP2A) and sperm-associated antigen 5 (SPAG5), these regulatory factors regulated by *TROAP* depend on CDC20 for their function. Therefore, CDC20 may be a key regulator of the *ASPM-TROAP* protumor pathway, and targeting CDC20 may weaken the tumor promoting effect.

ASPM as a useful cancer marker based on previous clinical case studies

To determine whether *TROAP* and ASMP have been reported in previous cancer-related studies, we searched NCBI for bioinformatic data, including ASMP and *TROAP*. Because *ASPM* is a downstream factor of *TROAP*, we used *ASPM* as an example to study its role in different cancer subtypes.

Case 1: Aromatase inhibitors (AIs) play an important role in the treatment of breast cancer. However, the efficacy rate of adjuvant therapy, including AI, is only 50–70%, and the efficacy rate declines when treating advanced disease. Researchers need accurate biomarkers to predict treatment response and determine which individuals will benefit from assisted AI therapy. In this study, researchers recorded the transcriptome changes of the patients before treatment, 2 weeks after the commencement of treatment, and 3 months after the commencement of treatment. We used *ASPM* as the standard for analysis (GSE59515). The results showed that, after 2 weeks of treatment, the expression of *ASPM* decreased significantly, but after 3 months of treatment, the expression of *ASPM* showed an upward trend (*Figure 7A*). This suggests that AI as an adjuvant therapy is most effective after 2 weeks. If the medication is continued,

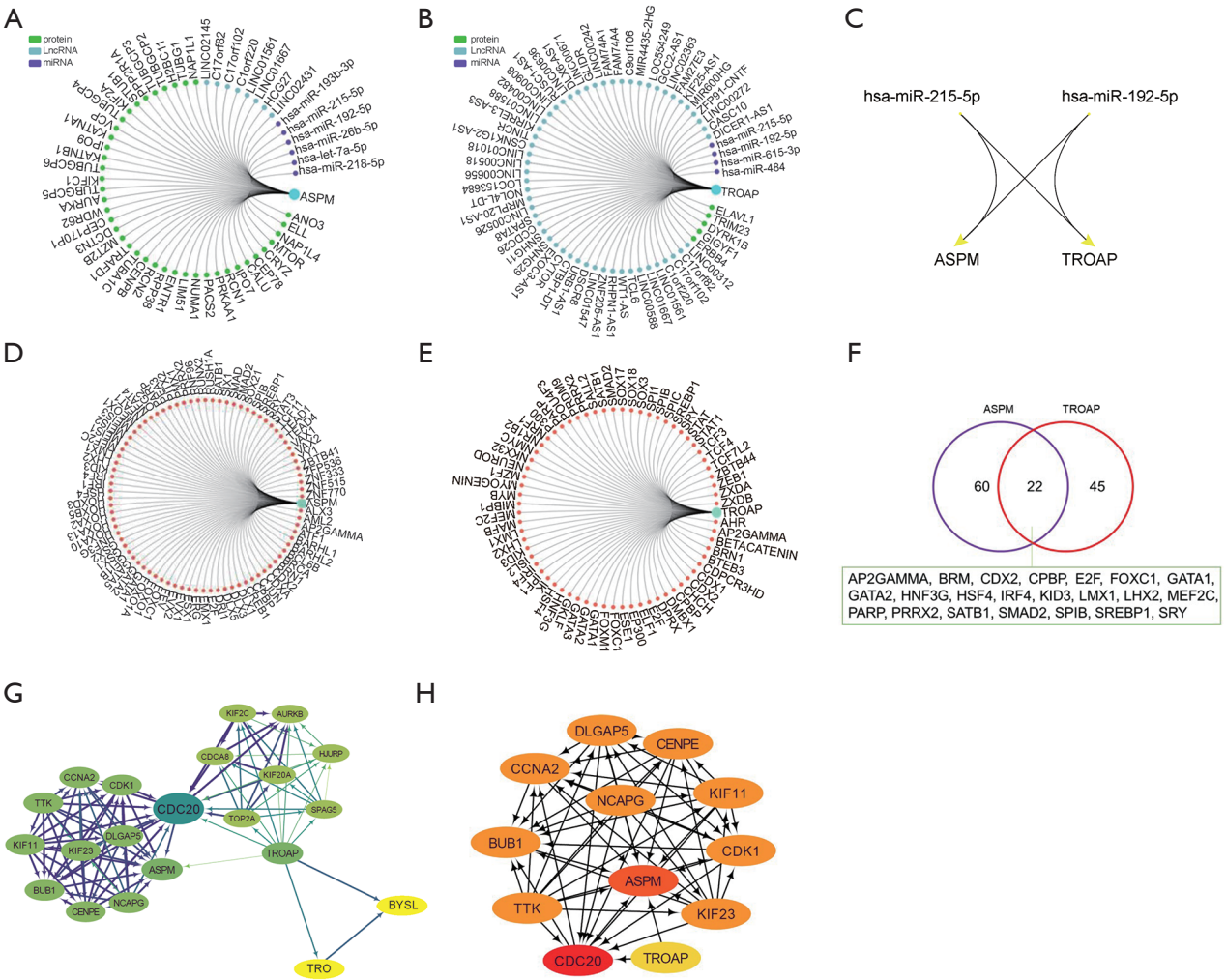

Figure 6 Regulatory network pathways of ASPM and TOARP. Regulatory factor interaction network of *ASPM* (A) and *TROAP* (B); miRNA regulatory factors shared by *ASPM* and *TROAP* (C); potential TFs of *ASPM* (D) and *TROAP* (E); Venn diagram of potential TFs shared by *ASPM* and *TROAP* (F); PPI analysis of *ASPM* and *TROAP* (G, H). *ASPM*, assembly factor for spindle microtubules; *TROAP*, trophinin-associated protein; lncRNA, long non-coding RNA; miRNA, microRNA; TF, transcription factor; PPI, protein-protein interaction network.

there will be no more significant therapeutic effect. Although the curative effect of AI is limited, the expression of *ASPM* still showed a nonsignificant downward trend compared with that before the medication, indicating that, even with long-term medication, AI itself will not aggravate the cancer process.

Case 2: Triple-negative breast cancer refers to cases in which the results of immunohistochemical examination of the cancer tissue are negative for estrogen receptor (ER), progesterone receptor (PR), and human epidermal growth factor receptor 2 (Her2) oncogene. This type of breast cancer accounts for 10.0% to 20.8% of all pathological types of breast cancer. It exhibits special biological behavior and clinicopathological characteristics and has a worse prognosis than other types. In this study, researchers extracted transcriptome samples of triple-negative breast cancer cells and normal breast duct cells. We analyzed the expression of *ASPM* in these cells (GSE38959). The results showed that the expression of *ASPM* in triple-negative breast cancer was significantly higher than that in normal breast duct cells (*Figure 7B*). This indicates that the high expression of *ASPM* is related to poor prognosis in this type of breast cancer.

Case 3: Tumor aggressiveness is one of the key indicators

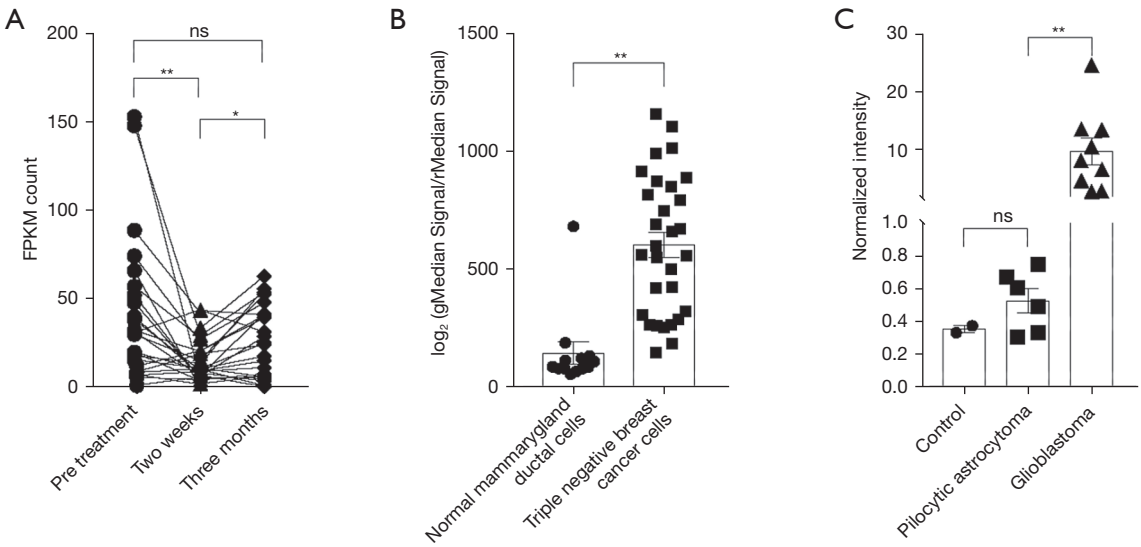

Figure 7 The expression of *ASPM* in different cancer subtypes: case 1 (A), case 2 (B), and case 3 (C). *ASPM*, assembly factor for spindle microtubules. *P<0.05, **P<0.01, ns: no significant.

of malignancy. In this study, researchers extracted the transcriptome data of highly aggressive glioblastoma and typical benign pilocytic astrocytoma and used normal cells as a control. We used *ASPM* as a malignant marker (GSE7330), and our results showed that the expression level of *ASPM* in highly aggressive glioblastoma was significantly higher than that in benign pilocytic astrocytoma. The latter and normal cells both had similar *ASPM* expression levels (*Figure 7C*). Therefore, *ASPM* as an indicator of malignant tumors may be related to the aggressiveness of tumor cells.

Discussion

Malignant tumors are significant threats to human life. Accurate markers help us understand the occurrence and development of malignant cancer and provide targets for achieving precise treatment. In this study, we used the TCGA database, the HPA database, and the GEPIA platform to screen *ASPM* and *TROAP*, two potential markers of cancers. Our results showed that these genes demonstrate malignant tumor marker characteristics in terms of RNA level, prognostic analysis, pathological protein level, and cell cycle changes.

The *TROAP* gene is a member of the housekeeping gene family, which has been reported to play a role in various tumors and cancers (12-14,34). Our results indicate that it is valuable as a new malignant cancer marker. The *ASPM* gene is the human ortholog of the *Drosophila* "abnormal spindle" gene (asp), which is responsible for the function of the mitotic spindle in embryonic neuroblasts (35,36). Studies in mice have shown that this gene plays a role in the regulation of the mitotic spindle and has a preferential role in the regulation of neurogenesis (37,38). Mutations in this gene are associated with primary type 5 microcephaly. Multiple transcript variants of this gene encoding different isoforms have been found. Therefore, this gene regulates the cell proliferation cycle, and the disorder caused by its high expression may cause the cell to eventually become cancerous (39,40). A previous study reported *ASPM*'s cancer-promoting effects but did not confirm its status as an oncogene. Our results prove this to a certain extent.

Although tumor cells have the ability to proliferate malignantly, their replication process also conforms to basic cell cycle principles. The spindle is an important element in the regulation of the cell cycle in eukaryotes (41,42). There are two main functions of the spindle in the cell cycle. One is to arrange and divide chromosomes. The integrity of the spindle determines the accuracy of chromosome division as well as the time and space of the division process. In addition, as chromosome division occurs, parts of the microtubules in the spindle do not divide to the poles along with the chromosome but rest in the center to form a central spindle. In the center of the spindle, the midbody is where two sets of microtubules of opposite polarities overlap, called the spindle midzone. These structures all ensure that the cell can divide properly. In recent years, there have

been many reports of abnormal spindles in cancer cells (43). In breast cancer, for example, spindle abnormalities serve as indicators of malignancy (44). Dysfunction of the spindle is often seen in malignant cancer cells, which theoretically cannot pass cell cycle checkpoints (45), but there are still unknown mechanisms that help the spindle enter the cell cycle through checkpoints. Our results show that *ASPM* and *TROAP* are involved in spindle function and may be key to helping abnormal spindles pass through cell cycle checkpoints.

The results of this study showed that *ASPM* and *TROAP* are strongly positively correlated, implying that these genes may interact with each other. The cell cycle analysis showed that *ASPM* and *TROAP* have similar expression profiles and high expression in the S&G2 phase. This suggests that these genes may promote tumor malignancy and development in the S&G2 phase of the cell cycle. Therefore, therapies targeting the *ASPM* and *TROAP* genes may be a potential treatment for malignant cancer.

Acknowledgments

Funding: This work was supported in part by the National Natural Science Foundation of China (No. 82072892), the Natural Science Foundation of Shanghai (No. 21ZR1454900), and the Key Discipline Project of Shanghai Jiading District (No. 2020-jdyxzdxk-13).

Footnote

Reporting Checklist: The authors have completed the STREGA reporting checklist. Available at https://atm.amegroups.com/article/view/10.21037/atm-22-1112/rc

Conflicts of Interest: All authors have completed the ICMJE uniform disclosure form (available at https://atm.amegroups.com/article/view/10.21037/atm-22-1112/coif). The authors have no conflicts of interest to declare.

Ethical Statement: The authors are accountable for all aspects of the work in ensuring that questions related to the accuracy or integrity of any part of the work are appropriately investigated and resolved. The study was conducted in accordance with the Declaration of Helsinki (as revised in 2013).

References

1. Feng RM, Zong YN, Cao SM, et al. Current cancer situation in China: good or bad news from the 2018 Global Cancer Statistics? Cancer Commun (Lond) 2019;39:22.
2. Bray F, Ferlay J, Soerjomataram I, et al. Global cancer statistics 2018: GLOBOCAN estimates of incidence and mortality worldwide for 36 cancers in 185 countries. CA Cancer J Clin 2018;68:394-424.
3. Blum A, Wang P, Zenklusen JC. SnapShot: TCGA-Analyzed Tumors. Cell 2018;173:530.
4. Uhlen M, Oksvold P, Fagerberg L, et al. Towards a knowledge-based Human Protein Atlas. Nat Biotechnol 2010;28:1248-50.
5. Clough E, Barrett T. The Gene Expression Omnibus Database. Methods Mol Biol 2016;1418:93-110.
6. Gao ZY, Yu F, Jia HX, et al. ASPM predicts poor prognosis and regulates cell proliferation in bladder cancer. Kaohsiung J Med Sci 2020;36:1021-9.
7. Feng Z, Zhang J, Zheng Y, et al. Overexpression of abnormal spindle-like microcephaly-associated (ASPM) increases tumor aggressiveness and predicts poor outcome in patients with lung adenocarcinoma. Transl Cancer Res 2021;10:983-97.
8. Yuan YJ, Sun Y, Gao R, et al. Abnormal spindle-like microcephaly-associated protein (ASPM) contributes to the progression of Lung Squamous Cell Carcinoma (LSCC) by regulating CDK4. J Cancer 2020;11:5413-23.
9. Jiang K, Rezabkova L, Hua S, et al. Microtubule minus-end regulation at spindle poles by an ASPM-katanin complex. Nat Cell Biol 2017;19:480-92.
10. Chen X, Huang L, Yang Y, et al. ASPM promotes glioblastoma growth by regulating G1 restriction point progression and Wnt-β-catenin signaling. Aging (Albany NY) 2020;12:224-41.
11. Yang S, Liu X, Yin Y, et al. Tastin is required for bipolar spindle assembly and centrosome integrity during mitosis. FASEB J 2008;22:1960-72.
12. Ye J, Chu C, Chen M, et al. TROAP regulates prostate cancer progression via the WNT3/survivin signalling

pathways. Oncol Rep 2019;41:1169-79.
13. Li K, Zhang R, Wei M, et al. TROAP Promotes Breast Cancer Proliferation and Metastasis. Biomed Res Int 2019;2019:6140951.
14. Hu H, Xu L, Chen Y, et al. The Upregulation of Trophinin-Associated Protein (TROAP) Predicts a Poor Prognosis in Hepatocellular Carcinoma. J Cancer 2019;10:957-67.
15. Lian Y, Fan W, Huang Y, et al. Downregulated Trophinin-Associated Protein Plays a Critical Role in Human Hepatocellular Carcinoma Through Upregulation of Tumor Cell Growth and Migration. Oncol Res 2018;26:691-701.
16. Schrock MS, Stromberg BR, Scarberry L, et al. APC/C ubiquitin ligase: Functions and mechanisms in tumorigenesis. Semin Cancer Biol 2020;67:80-91.
17. Wu F, Dai X, Gan W, et al. Prostate cancer-associated mutation in SPOP impairs its ability to target Cdc20 for poly-ubiquitination and degradation. Cancer Lett 2017;385:207-14.
18. Mao DD, Gujar AD, Mahlokozera T, et al. A CDC20-APC/SOX2 Signaling Axis Regulates Human Glioblastoma Stem-like Cells. Cell Rep 2015;11:1809-21.
19. Paul D, Ghorai S, Dinesh US, et al. Cdc20 directs proteasome-mediated degradation of the tumor suppressor SMAR1 in higher grades of cancer through the anaphase promoting complex. Cell Death Dis 2017;8:e2882.
20. Kidokoro T, Tanikawa C, Furukawa Y, et al. CDC20, a potential cancer therapeutic target, is negatively regulated by p53. Oncogene 2008;27:1562-71.
21. Stegmeier F, Rape M, Draviam VM, et al. Anaphase initiation is regulated by antagonistic ubiquitination and deubiquitination activities. Nature 2007;446:876-81.
22. Zhang Q, Huang H, Liu A, et al. Cell division cycle 20 (CDC20) drives prostate cancer progression via stabilization of β-catenin in cancer stem-like cells. EBioMedicine 2019;42:397-407.
23. Chu Z, Zhang X, Li Q, et al. CDC20 contributes to the development of human cutaneous squamous cell carcinoma through the Wnt/β catenin signaling pathway. Int J Oncol 2019;54:1534-44.
24. Szklarczyk D, Gable AL, Nastou KC, et al. The STRING database in 2021: customizable protein-protein networks, and functional characterization of user-uploaded gene/measurement sets. Nucleic Acids Res 2021;49:D605-12.
25. Shannon P, Markiel A, Ozier O, et al. Cytoscape: a software environment for integrated models of biomolecular interaction networks. Genome Res 2003;13:2498-504.
26. Pontén F, Jirström K, Uhlen M. The Human Protein Atlas--a tool for pathology. J Pathol 2008;216:387-93.
27. Ouyang W, Winsnes CF, Hjelmare M, et al. Analysis of the Human Protein Atlas Image Classification competition. Nat Methods 2019;16:1254-61.
28. Fu J, Wei C, He J, et al. Evaluation and characterization of HSPA5 (GRP78) expression profiles in normal individuals and cancer patients with COVID-19. Int J Biol Sci 2021;17:897-910.
29. Schafer KA. The cell cycle: a review. Vet Pathol 1998;35:461-78.
30. New insights into the regulation of cell cycle. J Mol Cell Biol 2018;10:1.
31. Benz C, Urbaniak MD. Organising the cell cycle in the absence of transcriptional control: Dynamic phosphorylation co-ordinates the Trypanosoma brucei cell cycle post-transcriptionally. PLoS Pathog 2019;15:e1008129.
32. Williams GH, Stoeber K. The cell cycle and cancer. J Pathol 2012;226:352-64.
33. Woynarowski JM, Woynarowska BA, Trevino AV, et al. Cell cycle effects and induction of premitotic apoptosis by irofulven in synchronized cancer cells. Cancer Biol Ther 2004;3:1137-42; discussion 1143-4.
34. Jiao Y, Li Y, Lu Z, et al. High Trophinin-Associated Protein Expression Is an Independent Predictor of Poor Survival in Liver Cancer. Dig Dis Sci 2019;64:137-43.
35. Bond J, Roberts E, Mochida GH, et al. ASPM is a major determinant of cerebral cortical size. Nat Genet 2002;32:316-20.
36. Zhong X, Liu L, Zhao A, et al. The abnormal spindle-like, microcephaly-associated (ASPM) gene encodes a centrosomal protein. Cell Cycle 2005;4:1227-9.
37. Vulcani-Freitas TM, Saba-Silva N, Cappellano A, et al. ASPM gene expression in medulloblastoma. Childs Nerv Syst 2011;27:71-4.
38. Williams SE, Garcia I, Crowther AJ, et al. Aspm sustains postnatal cerebellar neurogenesis and medulloblastoma growth in mice. Development 2015;142:3921-32.
39. Fujimori A, Itoh K, Goto S, et al. Disruption of Aspm causes microcephaly with abnormal neuronal differentiation. Brain Dev 2014;36:661-9.
40. Makhdoom EUH, Waseem SS, Iqbal M, et al. Modifier Genes in Microcephaly: A Report on WDR62, CEP63, RAD50 and PCNT Variants Exacerbating Disease Caused by Biallelic Mutations of ASPM and CENPJ. Genes (Basel) 2021;12:731.

41. Maiato H, Logarinho E. Mitotic spindle multipolarity without centrosome amplification. Nat Cell Biol 2014;16:386-94.
42. Choi JH, Ro JY. Cutaneous Spindle Cell Neoplasms: Pattern-Based Diagnostic Approach. Arch Pathol Lab Med 2018;142:958-72.
43. Pease JC, Tirnauer JS. Mitotic spindle misorientation in cancer--out of alignment and into the fire. J Cell Sci 2011;124:1007-16.
44. Carter MR, Hornick JL, Lester S, et al. Spindle cell (sarcomatoid) carcinoma of the breast: a clinicopathologic and immunohistochemical analysis of 29 cases. Am J Surg Pathol 2006;30:300-9.
45. Bharadwaj R, Yu H. The spindle checkpoint, aneuploidy, and cancer. Oncogene 2004;23:2016-27.

Cite this article as: Liu H, Zhou Q, Xu X, Du Y, Wu J. *ASPM* and *TROAP* gene expression as potential malignant tumor markers. Ann Transl Med 2022;10(10):586. doi: 10.21037/atm-22-1112

Supplementary

Table S1 The top 10 genes in each cancer type that related to poor prognosis based on the GEPIA results

Cancer type	Gene symbol	Gene ID	P value (survival OS)
ACC	*TROAP*	ENSG00000135451.12	7.67E-09
	EP400NL	ENSG00000185684.12	4.32E-08
	ASPM	ENSG00000066279.16	5.57E-08
	TICRR	ENSG00000140534.13	6.70E-08
	CDC20	ENSG00000117399.13	6.73E-08
	SPAG5	ENSG00000076382.16	7.49E-08
	MELK	ENSG00000165304.7	7.59E-08
	SPC24	ENSG00000161888.11	8.60E-08
	DNA2	ENSG00000138346.14	9.62E-08
	LRP5L	ENSG00000100068.11	1.03E-07
BLCA	*GSDMB*	ENSG00000073605.18	2.16E-07
	RP3-395M20.8	ENSG00000238164.6	3.26E-07
	IL9RP3	ENSG00000226942.2	5.40E-07
	HEYL	ENSG00000163909.7	6.68E-06
	RP11-488L18.10	ENSG00000259865.1	6.93E-06
	PCDH9	ENSG00000184226.14	8.32E-06
	EMP1	ENSG00000134531.9	1.00E-05
	WASH7P	ENSG00000226210.3	1.16E-05
	BCL2L14	ENSG00000121380.12	1.17E-05
	GXYLT2	ENSG00000172986.12	1.30E-05
BRCA	*HSPA8P1*	ENSG00000234176.1	1.71E-06
	DCTPP1	ENSG00000179958.8	3.16E-06
	RP11-727F15.9	ENSG00000256690.1	7.20E-06
	APOOL	ENSG00000155008.13	1.26E-05
	VDAC1P2	ENSG00000213856.3	1.37E-05
	IGHA2	ENSG00000211890.3	2.25E-05
	LRP11	ENSG00000120256.9	2.81E-05
	TARS	ENSG00000113407.13	2.88E-05
	AC137932.6	ENSG00000261253.2	5.09E-05
	FAM173B	ENSG00000150756.13	5.38E-05
CESC	*MTCP1*	ENSG00000214827.9	2.62E-06
	F8A1	ENSG00000277203.1	4.80E-06
	RP11-638I2.6	ENSG00000258504.2	5.79E-06
	EGLN1	ENSG00000135766.8	6.77E-06
	ESM1	ENSG00000164283.12	9.05E-06
	DDX49	ENSG00000105671.11	1.05E-05
	GS1-393G12.14	ENSG00000272115.1	1.14E-05
	AC092614.2	ENSG00000227542.1	1.31E-05

Table S1 *(continued)*

https://dx.doi.org/10.21037/atm-22-1112

Table S1 *(continued)*

Cancer type	Gene symbol	Gene ID	P value (survival OS)
	AGPAT4	ENSG00000026652.13	1.58E-05
	PRSS36	ENSG00000178226.10	2.03E-05
CHOL	*LINC01587*	ENSG00000082929.8	1.60E-04
	CTD-2033C11.1	ENSG00000269961.1	2.49E-04
	ZNF471	ENSG00000196263.7	7.74E-04
	RP11-775C24.3	ENSG00000260619.1	8.25E-04
	LMNTD2	ENSG00000185522.8	1.34E-03
	RP11-573D15.2	ENSG00000232233.1	1.65E-03
	DYM	ENSG00000141627.13	1.69E-03
	EIF5A	ENSG00000132507.17	1.73E-03
	EIF4EBP3	ENSG00000243056.1	1.80E-03
	COL4A3	ENSG00000169031.18	1.84E-03
COAD	*SUCLG2*	ENSG00000172340.14	2.00E-05
	FABP3	ENSG00000121769.7	9.74E-05
	MCCC1-AS1	ENSG00000243368.2	1.00E-04
	C5orf46	ENSG00000178776.4	1.01E-04
	NSUN6	ENSG00000241058.3	1.03E-04
	RPL32P3	ENSG00000251474.6	1.18E-04
	RP11-365O16.6	ENSG00000237101.1	1.24E-04
	ANKRD24	ENSG00000089847.12	1.59E-04
	RP3-475N16.1	ENSG00000231113.2	1.70E-04
	RP11-66B24.2	ENSG00000232386.9	2.08E-04
DLBC	*CYP4F11*	ENSG00000171903.16	2.27E-03
	SIGLEC15	ENSG00000197046.11	2.28E-03
	CFD	ENSG00000197766.7	2.70E-03
	PLCH1	ENSG00000114805.16	2.98E-03
	KLHDC3	ENSG00000124702.17	3.12E-03
	RP11-266K4.14	ENSG00000275367.1	3.42E-03
	FBXW9	ENSG00000132004.12	3.74E-03
	CENPBD1P1	ENSG00000213753.10	3.78E-03
	SYCP3	ENSG00000139351.14	4.74E-03
	CENPM	ENSG00000100162.14	4.85E-03
ESCA	*KCP*	ENSG00000135253.13	4.97E-04
	UFSP2	ENSG00000109775.10	6.88E-04
	ARHGAP4	ENSG00000089820.15	9.82E-04
	RP11-51J9.4	ENSG00000253708.1	1.21E-03
	XXbac-BPG246D15.9	ENSG00000250264.1	1.22E-03
	PRDX4	ENSG00000123131.12	1.32E-03

Table S1 *(continued)*

https://dx.doi.org/10.21037/atm-22-1112

Table S1 *(continued)*

Cancer type	Gene symbol	Gene ID	P value (survival OS)
	RP11-271K21.12	ENSG00000279147.1	1.52E-03
	RP11-430L17.1	ENSG00000226457.1	1.54E-03
	PIGA	ENSG00000165195.13	1.57E-03
	RP11-10E18.7	ENSG00000276809.1	1.58E-03
GBM	*LOXL1*	ENSG00000129038.15	2.54E-06
	LOXL1-AS1	ENSG00000261801.5	2.88E-06
	TSPAN4	ENSG00000214063.10	1.59E-05
	AC096574.4	ENSG00000225057.2	1.86E-05
	SAMD13	ENSG00000203943.8	2.53E-05
	NLRP12	ENSG00000142405.21	3.15E-05
	EPS8L2	ENSG00000177106.14	3.87E-05
	LINC01503	ENSG00000233901.5	4.01E-05
	MLPH	ENSG00000115648.13	4.04E-05
	RP11-539I5.1	ENSG00000225302.2	4.99E-05
HNSC	*JCHAIN*	ENSG00000132465.10	3.97E-07
	AL928768.3	ENSG00000253701.2	4.32E-07
	AIG1	ENSG00000146416.16	8.87E-07
	CRLF2	ENSG00000205755.10	9.99E-07
	MASP1	ENSG00000127241.16	1.28E-06
	KIAA1683	ENSG00000130518.16	3.30E-06
	ESD	ENSG00000139684.13	5.06E-06
	ZNF266	ENSG00000174652.17	6.43E-06
	LMX1B	ENSG00000136944.17	6.59E-06
	AC002066.1	ENSG00000237813.3	7.42E-06
KICH	*ARPC1A*	ENSG00000241685.8	1.27E-04
	NCAPG2	ENSG00000146918.19	1.67E-04
	ITGAE	ENSG00000083457.11	2.65E-04
	RAB27A	ENSG00000069974.15	2.88E-04
	LRWD1	ENSG00000161036.10	3.10E-04
	COX20	ENSG00000203667.9	3.28E-04
	TXNDC17	ENSG00000129235.10	3.33E-04
	RPUSD3	ENSG00000156990.14	3.67E-04
	RHNO1	ENSG00000171792.10	3.83E-04
	TIMELESS	ENSG00000111602.11	4.03E-04
KIRC	*SLC16A12*	ENSG00000152779.13	4.05E-13
	SGCB	ENSG00000163069.12	6.01E-13
	SOWAHB	ENSG00000186212.3	8.16E-13
	FBXL5	ENSG00000118564.14	1.21E-12

Table S1 *(continued)*

https://dx.doi.org/10.21037/atm-22-1112

Table S1 *(continued)*

Cancer type	Gene symbol	Gene ID	P value (survival OS)
	CRB3	ENSG00000130545.15	1.79E-12
	AR	ENSG00000169083.15	2.99E-12
	ALDH6A1	ENSG00000119711.12	4.82E-12
	MSH3	ENSG00000113318.9	4.98E-12
	PPM1A	ENSG00000100614.17	5.53E-12
	GNA11	ENSG00000088256.8	6.22E-12
KIRP	*CCNB2*	ENSG00000157456.7	2.55E-07
	TICRR	ENSG00000140534.13	3.43E-07
	CDK1	ENSG00000170312.15	3.55E-07
	DLGAP5	ENSG00000126787.12	7.23E-07
	NPTX2	ENSG00000106236.3	8.00E-07
	ASPM	ENSG00000066279.16	8.06E-07
	ATP5A1	ENSG00000152234.15	1.06E-06
	TPX2	ENSG00000088325.15	1.27E-06
	TBX18	ENSG00000112837.16	2.20E-06
	KIF18A	ENSG00000121621.6	2.82E-06
LAML	*STIM2*	ENSG00000109689.14	2.44E-07
	MRPL16	ENSG00000166902.4	1.41E-06
	ANKEF1	ENSG00000132623.15	2.52E-06
	DDIT4	ENSG00000168209.4	4.59E-06
	GRAMD1C	ENSG00000178075.19	5.23E-06
	SRP14-AS1	ENSG00000248508.6	6.31E-06
	PTP4A3	ENSG00000184489.11	8.58E-06
	KHDC1	ENSG00000135314.12	1.43E-05
	NTMT1	ENSG00000148335.14	1.91E-05
	LINC01480	ENSG00000270164.1	2.12E-05
LGG	*PTGFRN*	ENSG00000134247.9	2.22E-16
	WEE1	ENSG00000166483.10	3.33E-16
	RAB27A	ENSG00000069974.15	1.11E-15
	EMILIN1	ENSG00000138080.13	1.44E-15
	LATS2	ENSG00000150457.8	9.66E-15
	RAD54B	ENSG00000197275.12	1.13E-14
	EN1	ENSG00000163064.6	1.30E-14
	IGFBP2	ENSG00000115457.9	1.31E-14
	SPHKAP	ENSG00000153820.12	1.38E-14
	IGF2BP3	ENSG00000136231.13	2.70E-14
LIHC	*PTDSS2*	ENSG00000174915.11	1.82E-09
	PIGU	ENSG00000101464.10	1.09E-08

Table S1 *(continued)*

https://dx.doi.org/10.21037/atm-22-1112

Table S1 *(continued)*

Cancer type	Gene symbol	Gene ID	P value (survival OS)
	UCK2	ENSG00000143179.12	5.65E-08
	KPNA2	ENSG00000182481.8	7.20E-08
	HILPDA	ENSG00000135245.9	8.48E-08
	MED19	ENSG00000156603.14	1.34E-07
	GTPBP4	ENSG00000107937.18	1.80E-07
	RUVBL1	ENSG00000175792.11	1.86E-07
	CCT5	ENSG00000150753.11	1.90E-07
	KB-68A7.1	ENSG00000274225.1	2.01E-07
LUAD	*ANLN*	ENSG00000011426.10	5.47E-08
	FAM83A	ENSG00000147689.16	2.33E-07
	GNPNAT1	ENSG00000100522.8	4.11E-07
	PLK1	ENSG00000166851.14	6.05E-07
	PKP2	ENSG00000057294.13	6.16E-07
	RGS20	ENSG00000147509.13	8.36E-07
	SMS	ENSG00000102172.15	1.26E-06
	GAPDH	ENSG00000111640.14	1.76E-06
	LDHA	ENSG00000134333.13	2.22E-06
	DKK1	ENSG00000107984.9	2.43E-06
LUSC	*SGCA*	ENSG00000108823.15	1.60E-05
	RP11-535M15.1	ENSG00000224848.1	4.04E-05
	RETN	ENSG00000104918.7	4.18E-05
	FAM65A	ENSG00000039523.17	5.66E-05
	CLDN5	ENSG00000184113.9	8.44E-05
	CTD-2245F17.3	ENSG00000269051.5	8.91E-05
	RP11-76C10.5	ENSG00000256151.1	9.15E-05
	CST3	ENSG00000101439.8	9.88E-05
	SUGT1P2	ENSG00000213842.2	9.97E-05
	CCDC69	ENSG00000198624.12	1.03E-04
MESO	*TOP2A*	ENSG00000131747.14	1.49E-08
	UBE2C	ENSG00000175063.16	1.63E-08
	TROAP	ENSG00000135451.12	3.48E-08
	UBE2M	ENSG00000130725.7	3.95E-08
	NEK2	ENSG00000117650.12	5.53E-08
	UBE2SP2	ENSG00000224126.2	7.21E-08
	SGOL1	ENSG00000129810.14	8.04E-08
	RECQL4	ENSG00000160957.12	1.40E-07
	LRFN4	ENSG00000173621.8	1.49E-07
	CCNB1	ENSG00000134057.14	1.50E-07

Table S1 *(continued)*

https://dx.doi.org/10.21037/atm-22-1112

Table S1 *(continued)*

Cancer type	Gene symbol	Gene ID	P value (survival OS)
OV	*ACOT13*	ENSG00000112304.10	2.23E-05
	CCDC160	ENSG00000203952.9	2.58E-05
	RP11-418H16.1	ENSG00000281920.1	2.80E-05
	CMBL	ENSG00000164237.8	3.16E-05
	HLA-DOB	ENSG00000241106.6	3.93E-05
	ARHGEF38	ENSG00000236699.8	5.70E-05
	HCG14	ENSG00000224157.1	6.12E-05
	C2orf88	ENSG00000187699.10	1.03E-04
	UBD	ENSG00000213886.3	1.27E-04
	TYMSOS	ENSG00000176912.3	1.71E-04
PAAD	*SPRN*	ENSG00000203772.7	4.28E-07
	RP11-763B22.4	ENSG00000237343.1	5.35E-07
	MUC21	ENSG00000204544.5	1.01E-06
	SCOC-AS1	ENSG00000196951.10	1.55E-06
	NDUFA6-AS1	ENSG00000237037.9	2.06E-06
	CTD-2349P21.12	ENSG00000276250.1	3.03E-06
	RP11-111M22.4	ENSG00000272301.1	3.32E-06
	RP5-1112D6.8	ENSG00000272356.1	3.59E-06
	FAM196B	ENSG00000204767.3	4.51E-06
	RP11-411K7.1	ENSG00000236740.6	7.04E-06
PCPG	*CRHR2*	ENSG00000106113.18	8.09E-04
	ARHGAP39	ENSG00000147799.11	1.35E-03
	UBXN8	ENSG00000104691.14	1.55E-03
	HSPA8P1	ENSG00000234176.1	3.06E-03
	FOXD4L4	ENSG00000184659.5	3.25E-03
	CTD-2371O3.3	ENSG00000268403.2	3.92E-03
	AC005104.3	ENSG00000223374.1	4.20E-03
	RP11-482D24.3	ENSG00000257918.1	4.37E-03
	DLEU2	ENSG00000231607.8	4.47E-03
	RP11-277P12.20	ENSG00000245648.1	6.05E-03
PRAD	*PFAS*	ENSG00000178921.13	8.89E-04
	TEX30	ENSG00000151287.16	1.13E-03
	MIS18BP1	ENSG00000129534.13	1.27E-03
	RP11-23J9.5	ENSG00000254876.5	1.31E-03
	SMG1P2	ENSG00000205534.6	1.37E-03
	SLC35E1P1	ENSG00000238286.1	1.64E-03
	WDR48	ENSG00000114742.13	1.82E-03
	ARHGAP19	ENSG00000213390.10	1.95E-03

Table S1 *(continued)*

https://dx.doi.org/10.21037/atm-22-1112

Table S1 *(continued)*

Cancer type	Gene symbol	Gene ID	P value (survival OS)
	PNRC2	ENSG00000189266.11	2.04E-03
	WDR11	ENSG00000120008.15	2.11E-03
READ	*PTPRVP*	ENSG00000243323.5	1.12E-05
	SIRT5	ENSG00000124523.14	3.54E-05
	RP3-486I3.7	ENSG00000237021.2	3.91E-05
	KCTD21-AS1	ENSG00000246174.7	7.64E-05
	RP3-486I3.4	ENSG00000233558.1	9.69E-05
	AC097523.1	ENSG00000233045.1	1.27E-04
	ZSCAN16	ENSG00000196812.4	1.33E-04
	RP11-379B18.5	ENSG00000241288.7	1.77E-04
	CTD-2623N2.3	ENSG00000267370.1	1.94E-04
	XXbac-BPGBPG55C20.2	ENSG00000272316.1	1.98E-04
SARC	*B3GALT4*	ENSG00000235863.3	3.26E-07
	ALDH1A1	ENSG00000165092.12	2.37E-06
	ADIRF	ENSG00000148671.13	4.86E-06
	NUDT7	ENSG00000140876.11	4.87E-06
	FZD2	ENSG00000180340.6	7.68E-06
	DHRS12	ENSG00000102796.10	9.85E-06
	GLO1	ENSG00000124767.6	1.20E-05
	RP11-395G23.3	ENSG00000254615.2	1.29E-05
	HNMT	ENSG00000150540.13	1.39E-05
	BCL2L14	ENSG00000121380.12	1.57E-05
SKCM	*NMI*	ENSG00000123609.10	1.84E-10
	GBP2	ENSG00000162645.12	7.04E-10
	TIMD4	ENSG00000145850.8	3.10E-09
	UBA7	ENSG00000182179.10	3.14E-09
	GBP4	ENSG00000162654.8	3.39E-09
	CD274	ENSG00000120217.13	6.18E-09
	ZBP1	ENSG00000124256.14	7.18E-09
	SEMA4D	ENSG00000187764.11	8.03E-09
	LAX1	ENSG00000122188.12	1.20E-08
	RP11-284N8.3	ENSG00000259834.1	1.47E-08
STAD	*FLJ16779*	ENSG00000275620.1	3.47E-06
	AC002480.3	ENSG00000232759.1	7.80E-06
	NRP1	ENSG00000099250.17	1.33E-05
	C6	ENSG00000039537.13	1.46E-05
	C8orf46	ENSG00000169085.11	1.58E-05
	PRTG	ENSG00000166450.12	4.52E-05

Table S1 *(continued)*

https://dx.doi.org/10.21037/atm-22-1112

Table S1 *(continued)*

Cancer type	Gene symbol	Gene ID	P value (survival OS)
	MAGED4	ENSG00000154545.16	4.59E-05
	PLCL1	ENSG00000115896.15	4.61E-05
	KIAA1462	ENSG00000165757.8	6.55E-05
	ITIH3	ENSG00000162267.12	6.67E-05
TGCT	*RP11-445F12.1*	ENSG00000277268.1	7.55E-06
	NBEAL2	ENSG00000160796.16	8.29E-05
	PM20D1	ENSG00000162877.12	9.79E-05
	AC090616.2	ENSG00000214708.4	2.02E-04
	THBS4	ENSG00000113296.14	2.81E-04
	CCDC28B	ENSG00000160050.14	7.79E-04
	PPIAP29	ENSG00000214975.4	8.36E-04
	GCM2	ENSG00000124827.6	9.40E-04
	CTC-471J1.2	ENSG00000260160.1	9.46E-04
	TOPAZ1	ENSG00000173769.4	1.05E-03
THCA	*RP13-580B18.4*	ENSG00000279072.1	1.49E-04
	SYNDIG1	ENSG00000101463.5	1.89E-04
	RP11-295P9.8	ENSG00000268549.1	2.38E-04
	NLGN3	ENSG00000196338.12	3.77E-04
	FBRSL1	ENSG00000112787.12	3.78E-04
	CACNB4	ENSG00000182389.18	3.91E-04
	GJB4	ENSG00000189433.5	4.30E-04
	LA16c-329F2.2	ENSG00000275092.1	4.48E-04
	PCDH19	ENSG00000165194.14	5.07E-04
	SIX2	ENSG00000170577.7	5.48E-04
THYM	*RP13-580B18.4*	ENSG00000279072.1	1.49E-04
	SYNDIG1	ENSG00000101463.5	1.89E-04
	RP11-295P9.8	ENSG00000268549.1	2.38E-04
	NLGN3	ENSG00000196338.12	3.77E-04
	FBRSL1	ENSG00000112787.12	3.78E-04
	CACNB4	ENSG00000182389.18	3.91E-04
	GJB4	ENSG00000189433.5	4.30E-04
	LA16c-329F2.2	ENSG00000275092.1	4.48E-04
	PCDH19	ENSG00000165194.14	5.07E-04
	SIX2	ENSG00000170577.7	5.48E-04
UCEC	*EFCAB6*	ENSG00000186976.14	1.79E-04
	HGS	ENSG00000185359.12	3.86E-04
	DSCAML1	ENSG00000177103.13	4.65E-04
	C12orf45	ENSG00000151131.9	4.87E-04

Table S1 *(continued)*

https://dx.doi.org/10.21037/atm-22-1112

Table S1 *(continued)*

Cancer type	Gene symbol	Gene ID	P value (survival OS)
	PKDREJ	ENSG00000130943.6	5.56E-04
	TPTEP1	ENSG00000100181.21	6.37E-04
	DGCR6	ENSG00000183628.12	6.87E-04
	GREB1	ENSG00000196208.13	7.27E-04
	WIF1	ENSG00000156076.9	8.53E-04
	MAOB	ENSG00000069535.13	9.04E-04
UCS	*HIST1H1C*	ENSG00000187837.3	1.23E-04
	PDE4A	ENSG00000065989.15	1.60E-04
	CBX5	ENSG00000094916.13	3.30E-04
	SCNN1G	ENSG00000166828.2	4.07E-04
	ZNF835	ENSG00000127903.13	5.21E-04
	RP11-276H19.2	ENSG00000269994.1	7.50E-04
	GUSBP4	ENSG00000239650.4	8.98E-04
	PXN-AS1	ENSG00000255857.5	9.90E-04
	HIST1H2AC	ENSG00000180573.9	1.12E-03
	CHGA	ENSG00000100604.12	1.13E-03
UVM	*TYMP*	ENSG00000025708.12	3.12E-07
	RP11-620J15.4	ENSG00000273805.1	3.90E-07
	RP11-599J14.2	ENSG00000256673.1	7.73E-07
	XXbac-B135H6.15	ENSG00000237476.1	1.37E-06
	SIRPG	ENSG00000089012.14	2.02E-06
	RP5-884G6.2	ENSG00000228084.1	2.04E-06
	GLA	ENSG00000102393.9	2.07E-06
	HLA-DMA	ENSG00000204257.14	2.23E-06
	CITED1	ENSG00000125931.10	2.30E-06
	ANPEP	ENSG00000166825.13	2.32E-06

OS, overall survival; ACC, adrenocortical carcinoma; BLCA, bladder urothelial carcinoma; BRCA, breast invasive carcinoma; CESC, cervical squamous cell carcinoma and endocervical adenocarcinoma; CHOL, cholangio carcinoma; COAD, colon adenocarcinoma; DLBC, lymphoid neoplasm diffuse large B-cell lymphoma; ESCA, esophageal carcinoma; GBM, glioblastoma multiforme; HNSC, head and neck squamous cell carcinoma; KICH, kidney chromophobe; KIRC, kidney renal clear cell carcinoma; KIRP, kidney renal papillary cell carcinoma; LAML, acute myeloid leukemia; LGG, brain lower grade glioma; LIHC, liver hepatocellular carcinoma; LUAD, lung adenocarcinoma; LUSC, lung squamous cell carcinoma; OV, ovarian serous cystadenocarcinoma; PAAD, pancreatic adenocarcinoma; PCPG, pheochromocytoma and paraganglioma; PRAD, prostate adenocarcinoma; READ, rectum adenocarcinoma; SARC, sarcoma; SKCM, skin cutaneous melanoma; STAD, stomach adenocarcinoma; TGCT, testicular germ cell tumors; THCA, thyroid carcinoma; THYM, thymoma; UCEC, uterine corpus endometrial carcinoma; UCS, uterine carcinosarcoma; UVM, uveal melanoma.

https://dx.doi.org/10.21037/atm-22-1112

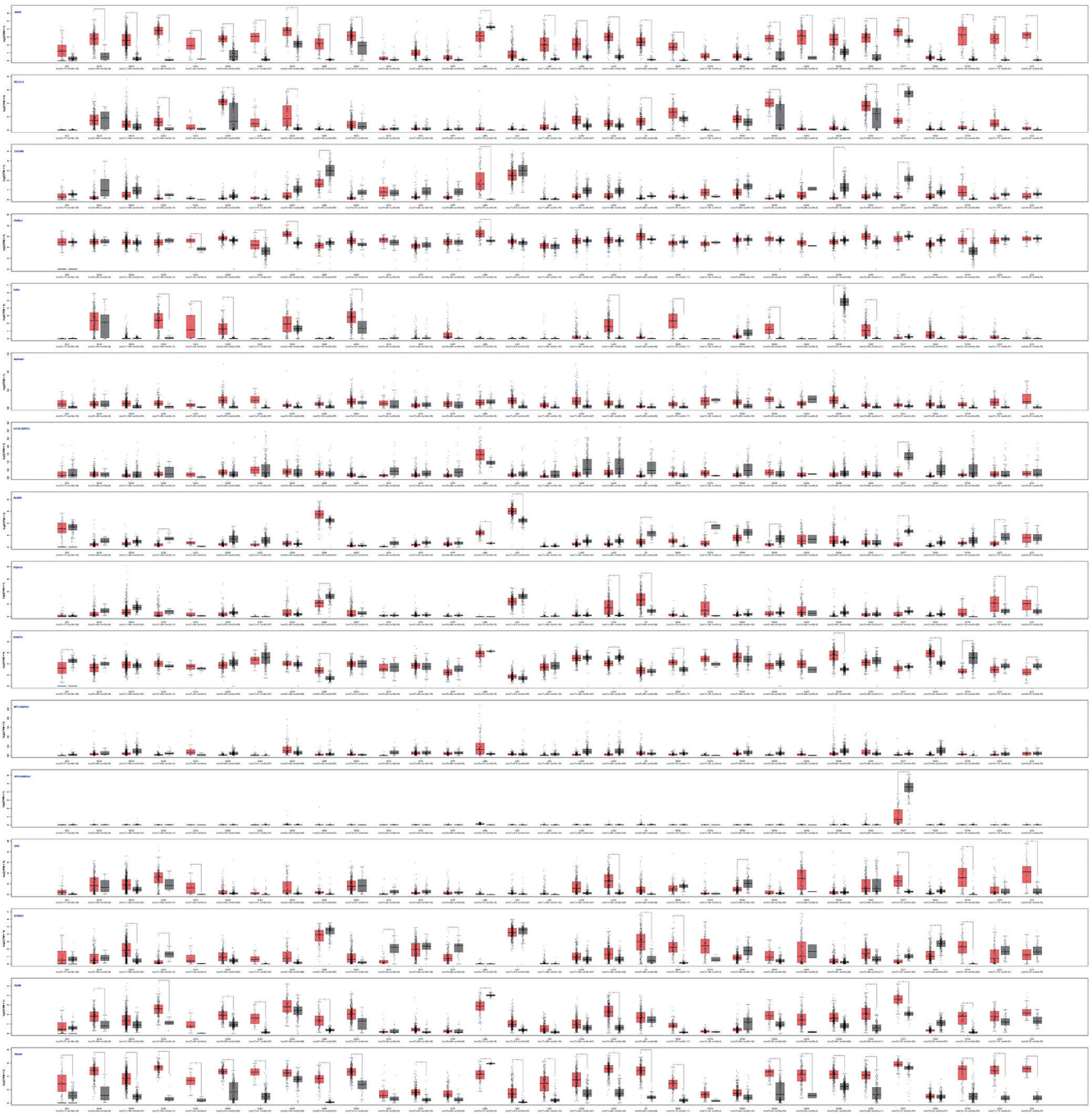

Figure S1 The expression of 16 most expressed genes in 31 types of cancers paired with normal tissues. T, tumor; N, normal. ACC, adrenocortical carcinoma; BLCA, bladder urothelial carcinoma; BRCA, breast invasive carcinoma; CESC, cervical squamous cell carcinoma and endocervical adenocarcinoma; CHOL, cholangio carcinoma; COAD, colon adenocarcinoma; DLBC, lymphoid neoplasm diffuse large B-cell lymphoma; ESCA, esophageal carcinoma; GBM, glioblastoma multiforme; HNSC, head and neck squamous cell carcinoma; KICH, kidney chromophobe; KIRC, kidney renal clear cell carcinoma; KIRP, kidney renal papillary cell carcinoma; LAML, acute myeloid leukemia; LGG, brain lower grade glioma; LIHC, liver hepatocellular carcinoma; LUAD, lung adenocarcinoma; LUSC, lung squamous cell carcinoma; OV, ovarian serous cystadenocarcinoma; PAAD, pancreatic adenocarcinoma; PCPG, pheochromocytoma and paraganglioma; PRAD, prostate adenocarcinoma; READ, rectum adenocarcinoma; SARC, sarcoma; SKCM, skin cutaneous melanoma; STAD, stomach adenocarcinoma; TGCT, testicular germ cell tumors; THCA, thyroid carcinoma; THYM, thymoma; UCEC, uterine corpus endometrial carcinoma; UCS, uterine carcinosarcoma. *P<0.05.

https://dx.doi.org/10.21037/atm-22-1112